Published in final edited form as:
Geophys Res Lett. 2019 July 16; 46(13): 7643–7653. doi:10.1029/2019gl083469.

Changes in Fire Activity in Africa from 2002 to 2016 and Their Potential Drivers

Maria Zubkova[1], **Luigi Boschetti**[1], **John T. Abatzoglou**[2], **Louis Giglio**[3]

[1]Department of Natural Resources and Society, University of Idaho, Moscow, ID, USA

[2]Department of Geography, University of Idaho, Moscow, ID, USA

[3]Department of Geographical Sciences, University of Maryland, College Park, MD, USA

Abstract

While several studies have reported a recent decline in area burned in Africa, the causes of this decline are still not well understood. In this study, we found that from 2002 to 2016 burned area in Africa declined by 18.5%, with the strongest decline (80% of the area) in the Northern Hemisphere. One third of the reduction in burned area occurred in croplands, suggesting that changes in agricultural practices (including cropland expansion) are not the predominant factor behind recent changes in fire extent. Linear models that considered interannual variability in climate factors directly related to biomass productivity and aridity explained about 70% of the decline in burned area in natural land cover. Our results provide evidence that despite the fact that most fires are human-caused in Africa, increased terrestrial moisture during 2002–2016 facilitated declines in fire activity in Africa.

Plain Language Summary

The last 15 years of satellite observations indicate a decrease of the global amount of burned area, but this decrease is not evenly distributed geographically. Africa, the continent most affected by fire, has seen the most pronounced decline in burned area. The causes are still poorly understood: the reduction in fire activity could be both due to changes in climate and human factors. We show that only about a third of the reduction in area burned occurred in croplands. The interannual burned area variability in natural lands (forest and nonforest) was linked to climate variables related to moisture availability. We found that about 70% of the reduction of area burned in natural lands can be explained by observed increase in plant-available moisture over the last 15 years. The results point to increased effective precipitation that inhibits flammability, ignition, and fire propagation, especially in wet savannas. These results bring new evidence that, in the complex

Correspondence to: M. Zubkova, mzubkova@uidaho.edu.

Supporting Information:
- Supporting Information S1
- Table S1
- Table S5
- Table S6

fire-climate-human relationship, both increased human pressure and changing climate patterns influenced recent fire activity trends in Africa.

1. Introduction

Several recent studies have reported a global decline in burned area, prominently observed in Africa (Andela et al., 2017; Earl & Simmonds, 2018). Africa is the most fire prone continent, responsible for over half of the global area burned and for more than half of the global pyrogenic greenhouse gas emissions (Rabin et al., 2015; Van der Werf et al., 2017). According to satellite-derived estimates, over 80% of burned area (BA) in Africa occurs in savanna with the remainder occurring in forests and croplands (Giglio et al., 2013). Fire seasonality in Africa follows the respective dry seasons occurring primarily from October to March with a peak of the season in December–January for Northern Hemisphere (NH), and April to October with a peak in August for Southern Hemisphere (SH; Boschetti & Roy, 2008). Savanna fires in Africa are generally surface fires, burning as frequently as every 1–6 years (Archibald, Scholes, Roy, et al., 2010; 2013). The long dry season of African savannas and the high rate of fuel accumulation have been identified as the main contributors of such an extensive amount of burning (Archibald et al., 2009); grasses can regrow quickly after the fire, which makes the ecosystem prone to frequent fires (Archibald et al., 2009; Van Wilgen & Scholes, 1997).

Three components must be present for fire ignition: sufficient biomass to burn, fuel flammability, and an ignition source (Bradstock, 2010; Moritz et al., 2012). Both climate and humans can modify biomass abundance, the number of ignitions, and potential fire spread. It is challenging to decouple the effect of these drivers, especially in Africa, a continent where humans have influenced the fire regime for millennia and where up to 90% of fires might be anthropogenic (Andela et al., 2017; Archibald, 2016; Knowles et al., 2016). Precipitation has a strong impact on the amount of BA in Africa (Andela & van der Werf, 2014; Archibald, Nickless, Govender, et al., 2010), but the relationship between fire activity and moisture availability is highly variable and ecosystem dependent (Abatzoglou et al., 2018; Williams & Abatzoglou, 2016). In fuel-limited ecosystems, precipitation promotes fuel load accumulation and subsequent fires, while in energy-limited ecosystems, precipitation enhances fuel moisture and limits flammability and fire spread (e.g., Daniau et al., 2012; Murphy et al., 2011). Additionally, several studies have confirmed that climatic variables related to water balance specific to vegetation demands, and therefore fuel moisture, have stronger and more direct relationships with fire activity compared to precipitation (e.g., Barbero et al., 2015; Daniau et al., 2012; Riley et al., 2013). The impact of human activities on fire is inherently complex, with direct and indirect effects. Increased population can directly result in increased ignitions, fire suppression, as well as altered fire seasonality (e.g., Balch et al., 2017). Indirectly, human activities lead to reductions of fuel amount and fuel connectivity due to livestock pressure, cropland expansion, and road density (Archibald, 2016). Anthropic influences on fire also vary geographically. For example, fire has long been used as a land management tool in much of Africa; fire is widely used for preparing agricultural fields, preventing bush encroachment, improving quality and quantity

of forage, maintaining biodiversity, hunting, and reducing future fire risk (Knowles et al., 2016; Le Page et al., 2010).

Previous studies have used empirical climate-fire models (Andela et al., 2017; Andela & van der Werf, 2014; Earl & Simmonds, 2018) to elucidate drivers of recent changes in fire activity in Africa. While the BA interannual variability in SH was partly explained by rainfall variability (Andela & van der Werf, 2014), the nature of the strong BA decline in NH is still not well understood. Earl and Simmonds (2018) proposed that it is linked to the observed increase of net primary productivity. This increase in net primary productivity in Africa was attributed to decrease in vapor pressure deficit (Zhao & Running, 2010) and increase in rainfall (Hoscilo et al., 2014). We hypothesize that increased fuel moisture reduced flammability and BA. Andela and van der Werf (2014) pointed at socio-economical changes as a main factor of reduction in BA NH Africa; however, their statistical models showed that only a quarter of the decline was attributed to cropland expansion and another quarter to changes in precipitation, leaving the remaining half of the reduction unexplained.

In the present study we reanalyzed the recent changes in fire activity in Africa using the MODIS MCD64A1 Burned Area product over a 15-year study period (2002–2016). Previous studies have typically calculated trends and variability in fire activity using high spatial resolution grids, possibly at a scale too fine to appropriately describe top-down climate-fire relationships on interannual time scales. Furthermore, they did not distinguish the influence of climate on fuel abundance and flammability for different vegetation types (Littell et al., 2016). We analyzed trends at the ecoregion scale and further examined changes within cropland and natural lands. Further, we expand on previous work by systematically exploring a simple relationship between the amount of burned area and climate, considering not only precipitation but also variables that are more mechanistically related to plant-available water and flammability. The overarching goal of this study is to investigate the drivers of trends and interannual variability in fire activity in Africa which will be useful for fire policies and management, and statistical fire and vegetation models.

2. Materials and Methods

2.1. Data Sets

Burned area: the most recent Collection 6 MODIS Global Burned Area Product (MCD64A1) provides daily global 500-m resolution BA maps (Giglio et al., 2018). The MCD64A1 data record from April 2002 to March 2017 was used to derive a monthly BA time series. Although the MODIS fire products are available from April 2000 onward, their use prior to November 2000 and during June 2001 is deprecated because of extended outages (Giglio et al., 2016).

Climate variables: the choice of an appropriate climate data set is vital but challenging, particularly in Africa where the lack of a dense weather station network severely affects data reliability (Dinku et al., 2014; Tadesse et al., 2014; Toté et al., 2015) especially for precipitation (Beck, 2017). We chose the Famine Early Warning Systems Network Land Data Assimilation System (FLDAS) since it was produced specifically for drought monitoring in Africa (McNally et al., 2017), and incorporates precipitation data from

infrared satellite observations, atmospheric models, and stations. We used simulation run "C" that used Noah Land Surface Model and outputs from MERRA-2 (Modern-Era Retrospective Analysis for Research and Applications) at 0.5° resolution (Rienecker et al., 2011) and Climate Hazards Group InfraRed Precipitation with Station data at 0.1° resolution (Funk et al., 2015) which has been extensively used in Africa (Dembélé & Zwart, 2016; Funk et al., 2015; Toté et al., 2015). Additionally, overall trends in precipitation and surface soil moisture derived from FLDAS agree with independent satellite-derived trends from Gravity Recovery and Climate Experiment (GRACE) 2002–2016 that depicts increased terrestrial water storage across much of Africa (Rodell et al., 2018), thus further supporting our choice of precipitation data set. From FLDAS we considered precipitation (P) and soil moisture content at 0- to 10-cm depth (SM). Penman-Monteith reference evapotranspiration data (ET_0) was derived from MERRA-2 for consistency, being one of the FLDAS inputs. Effective Rainfall (ER) was calculated as P minus ET_0. Monthly P, ER, and SM time series were generated from January 2001 to March 2017.

Global ecoregions:	The Terrestrial Ecoregions Of the World (Olson et al., 2001) were used as the spatial analysis unit, because of commonalities in vegetation which mediates climate-fire relationships as in previous studies (e.g., Abatzoglou et al., 2018).
Land cover:	The Land Cover Climate Change Initiative (LC-CCI) v.1.6.1 Annual Global Land Cover (2002–2015) was used to mask unburnable surfaces and to define land cover types within ecoregions. The LC-CCI 300-m resolution maps are generated from MERIS, PROBA-V, SPOT-VGT, and AVHRR data (CCI-LC, 2017).
Livestock density:	Gridded Livestock of the World (GLW 3) global subnational livestock distribution data for 2010 at 0.083333° (Gilbert et al., 2018). Densities of different livestock species were combined into actual carrying capacity (ACC) defined in equivalent tropical livestock units, applying the conversion factors for cattle (0.70), sheep, and goats (0.10) proposed by Pica-Ciamarra et al. (2007).
Road density:	Global Roads Inventory Project global gridded road density data set at 8-km resolution (Meijer et al., 2018).

2.2. Analysis

For the purpose of the analysis, Terrestrial Ecoregions Of the World and LC-CCI were used to create a two-level stratification, separating ecoregions by broad land cover types (forests, nonforest, and cropland). In this study, savannas, shrublands, and grasslands were aggregated into the nonforest class; croplands include all LC-CCI cropland and cropland-natural vegetation mosaic classes.

2.2.1. Burned Area Seasonality and Trends—Total BA was summarized using the April-to-March optimal fire year proposed by Boschetti and Roy (2008). This resulted in a 15-year annual BA time series stratified by land cover and ecoregion. Ecoregions where a land cover is not significantly present (i.e., less than 5% of the ecoregion area) and/or with negligible fire activity (less than 0.5% of the ecoregion burned on average) were excluded from the analysis. For each ecoregion, the fire season (FS) was determined as the minimum number of consecutive months in which 80% of the total average annual BA occurs (Abatzoglou et al., 2018).

In order to determine spatial patterns and rates of change, BA trends were calculated for each ecoregion by fitting a simple linear regression to the 15-year BA time series; trends were thus represented by the slope of the regression line.

2.2.2. Analysis of Potential Anthropogenic Drivers—Human activity has both the potential of increasing fire activity, through accidental and intentional ignitions, and decreasing it by transforming natural land into croplands, reducing fuel load through grazing, and due to landscape fragmentation (Archibald, 2016; Knowles et al., 2016). The lack of gridded, multitemporal data sets of variables directly linked to human pressure limits the possibility of including anthropogenic drivers in a continental fire model. As an alternative, we created spatial masks of (a) croplands, (b) grazing pressure, and (c) road density, and analyzed separately the BA trends inside and outside the areas affected by significant human activity.

2.2.2.1. Croplands: In order to fully account for cropland expansion during the study period, we aggregated the annual land cover maps to define a single cropland mask encompassing any pixel mapped as cropland or cropland/natural vegetation mosaic during 2002–2016. This choice ensures that the burned area trends observed inside the cropland mask fully capture both cropland expansion and any changes in agricultural practices, whereas the trends observed outside of the mask reflect only areas that remain natural lands for the entire time period.

2.2.2.2. Grazing Pressure: Grazing negatively influences fire activity, since livestock reduces available fuel (Anderson et al., 2007; Archibald et al., 2009; Archibald & Hempson, 2016). Spatial analyses have observed that BA in SH Africa is drastically reduced when ACC is greater than six tropical livestock units, but relationships between grazing pressure and area burned are nonlinear since more grazers are required to reduce fuel loads in more productive ecosystems (Archibald et al., 2009; Archibald & Hempson, 2016). To account for the different agroecological conditions across Africa, we followed the methods proposed by Pica-Ciamarra et al. (2007), using reference Maximum Carrying Capacity values provided for different levels of annual rainfall and defining four grazing pressure classes based on the ratio between the ACC from the GLW3 data set and Maximum Carrying Capacity (Table S2 in the supporting information).

2.2.2.3. Road Density: We defined a map of high/low road density by applying to the Global Roads Inventory Project data set the threshold value of 33.3 m/km^2 after which BA significantly decreases, as proposed by Archibald et al. (2009).

2.2.3. Fire-Climate Relationship—We investigated the relationship between fire and climate on natural lands (i.e., excluding all croplands as defined above) using ecoregion-level linear models that predict BA as a function of climate variables, temporally integrated over meaningful intervals that represent conditions prior to and during the FS.

Three climate variables (*P*, *ER*, and *SM*) were considered because previous studies found them to be strong predictors of fire activity and drought in forest and savanna (Daniau et al., 2013; Higuera et al., 2015; Lehmann et al., 2014; McNally et al., 2017). Previous studies

showed that the relationship between fire and climate can be sensitive to the seasonal windows examined (Littell et al., 2016); we therefore considered distinct temporal accumulation intervals that capture the conditions both antecedent to the FS and concurrent with the FS which encompass the influence of climate variability on fuel loading and flammability, respectively. The average monthly value of each variable was calculated for each ecoregion, and integrated for each year over two temporal intervals: the FS, and the water year preceding the fire season (1WY), defined as the 12-month period ending 2 months before the FS (Abatzoglou et al., 2018).

The relative importance of antecedent and concurrent conditions changes across ecosystems. For example, in fuel-limited ecosystems, like SH nonforest, antecedent moisture is the main driver of fire activity, because it promotes biomass accumulation and therefore increases the amount of available fuel to support subsequent fires (Archibald, Nickless, Scholes, et al., 2010; Balfour & Howison, 2001; Van Wilgen et al., 2004). In energy-limited systems, like tropical forests, unusually dry conditions during the FS promote fire activity because of increased flammability (Cochrane, 2003; Higuera et al., 2015; Littell et al., 2016).

Expanding on the approach by Abatzoglou et al. (2018), for each ecoregion the relationship between BA and climate time series was explored through a simple linear model. BA was log-transformed to satisfy the assumption of normality as BA data are often right skewed (Abatzoglou et al., 2018; Higuera et al., 2015). Thus, the base-10 logarithm of the annual BA (BA_{LC}) in each land cover type (forest, nonforest) of each ecoregion is predicted as the linear combination of antecedent (C1) and concurrent (C2) climate conditions, plus an error term ε:

$$\log(BA_{LC}) = \beta_0 + \beta_1 \times C1 + \beta_2 \times C2 + \varepsilon \quad (1)$$

The model (1) was built separately for the three climate variables to evaluate the robustness of relationships and test whether measures of surface moisture that are more mechanistically related to plant-available moisture improve upon those which only consider precipitation; in each case, β_0, β_1, and β_2 were estimated through ordinary least squares, and the time series of predicted BA (BA_{pred}) was computed. The ratio $= \frac{t(\boldsymbol{BA}\mathbf{pred})}{t(\boldsymbol{BA})}$, between the slope t [Mha/year] of the linear interpolation of the predicted and observed BA time series is the fraction of BA trend that can be explained by the climate variables and represents the degree to which climate variables have driven BA changes in our model framework.

To verify the assumption of independence of covariance of the predictor variables, we computed the variance inflation factor (VIF), that quantifies the severity of multicollinearity of C1 and C2, with VIF > 5 being a common cutoff value for high collinearity (James et al., 2013).

We computed the Durbin-Watson statistic to assess the temporal autocorrelation (Durbin & Watson, 1950). Because in several ecoregions the test-confirmed temporal autocorrelation at 1 year lags, we also explored a modified version of (1) using the first-order differencing

procedure, which is one of the most common remedies for temporal autocorrelation (Chatfield, 1996; Wooldridge, 2013).

Given the relatively short time interval of the study, we verified the robustness of the analysis by testing the use of simplified versions of (version of (1), using for each ecoregion the single time interval that resulted in the largest adjusted coefficient of determination. Additionally, we repeated the analysis by using detrended climate and BA time series to fit the model, and then applying the model to the original time series.

3. Results

3.1. Burned Area Trends

During the study period, the annual average BA in Africa was 280.6 Mha, 45.7% of which was in NH. Of the 112 ecoregions, 81 had significant fire activity; the ecoregions excluded from the analysis are prevalently located around the Sahara Desert. Nonforest fires were predominant (204.7 Mha/year, 72.9% of the total), followed by forest fires (41.1 Mha/year, 14.7% of the total) and cropland fires (34.8 Mha/year, 12.4% of the total; (Figure 1, Table S1).

Overall, BA in Africa declined by 51.9 Mha (18.5%) during 2002–2016 with 80.3% of the decline (41.7 Mha) occurring in NH. Negative trends were statistically significant ($p < 0.05$) in 21 of the 81 ecoregions, 14 of which were in NH. Although several ecoregions showed a positive trend, none were statistically significant.

3.2. Impact of Human Factors on BA Trends

The cropland mask derived from the aggregation of the 2002–2015 LC-CCI annual maps encompassed a total of 491 Mha (Figure S2a), with only a modest expansion (1.06 Mha) observed in the study period. The interannual variability within natural lands and croplands is very similar (Figure 1, right column); since it is well established that climate explains most of fire interannual variabilities (Andela et al., 2017), this may imply that climate is responsible for years with high or low fire activity even in croplands. BA trends have the same direction but vary in magnitude, with cropland burning experiencing a steeper negative trend than natural land covers in both hemispheres. Overall, croplands account for 31.7% of the total BA decline (31.6% in NH, 32.0% in SH).

Livestock pressure (Figure S2b) highly correlates spatially with croplands (Figure S2a), with over 50% of the high livestock pressure areas falling within the cropland mask. We separately computed BA trends for each livestock pressure class on croplands and on natural lands (Table S3). Considering the whole continent, the negative trend is higher with some grazing pressure (−1.7% to −1.9% on natural lands, −4.6% to −4.7 % on croplands) than no grazing pressure (−0.8% on natural lands, −2.4% on croplands). The two hemispheres, however, exhibit a very different behavior, with a strong connection between livestock pressure and BA trends in SH both in croplands and natural lands, and a negligible connection in NH. In particular, about 75% of BA in NH, and the strongest negative trend (−1.9%/year which accounts for 78% of the BA decline), occurred in areas with no livestock pressure. Higher level of livestock pressure showed a very similar, albeit slightly lower trend

(−1.6%/year, −1.3%/year, and −1.6%/year for low, medium, and high pressure, respectively). These results suggest that part of the observed BA reduction in croplands could be attributed to grazing, but the decline of BA on natural lands in NH does not appear to be related to livestock pressure.

BA trends stratified by road density and land cover are reported in Table S4. At the continental level, high road density corresponds to a slightly more pronounced BA trend (−0.9% and −1.1% for low and high road density in natural lands, −3.0% and −3.3% in croplands), with a stronger relationship in SH than NH. In natural lands, in particular, the trend is −0.2% and −0.5% for low and high density in SH, while −1.7% and −1.9% in NH. These results suggest that in NH road density is not a likely driver of BA decline in natural lands.

3.3. Climate and BA Trends in Natural Lands

Increased ER and surface SM due to a combination of increased rainfall and decreased ETo have been observed across much of Africa in the last 15 years (Figure 2). BA in nonforest (Figure S4) negatively correlates with all three climate variables at concurrent (FS) and antecedent (1WY) time scales in Northern and Central Africa, and positively in Southern Africa but only at antecedent time scales. Noticeably, P has a weaker correlation with BA than ER and SM in all ecoregions. Considering forests instead (Figure S5), most of the ecoregions did not have a strong relationship between BA and either concurrent or antecedent climate conditions, and this relationship was predominantly negative.

The linear models (version of (1) were estimated for each ecoregion and land cover, separately for each climate variable (Tables S5 and S6). Only two ecoregions had VIF > 5, indicating that the use of C1 and C2 in (version of (1) is not redundant.

ER was the best predictor of the overall BA decline, explaining 73.2% of the observed trend, followed by SM (60.8 %) and P (30.1 %). SM, however, better reconstructed the interannual variability, resulting in slightly lower residuals (mean absolute error, MAE = 2.7%) than ER (MAE = 3.0%); P had instead significantly higher residuals (MAE = 4.2%). Considering separately the two hemispheres and the two land covers, in NH, ER was the best predictor in nonforest, with SM performing only marginally worse. While in NH in forest, SM was a better predictor. In SH there is no clear pattern, with all three variables performing similarly both in terms of trend and interannual variability. To summarize the results, Figure 3f reports the prediction obtained using the best variable for each ecoregion; Figure S6 shows the spatial distribution of the best climate predictor for each ecoregion. The results of the modified model using the first-order differencing procedure are presented for completeness as Figures S6–S10. Temporal autocorrelation was significant only in few ecoregions, and the results of the transformed models are consistent with the original models. The simplified version of the models (Figure S11) confirmed that ER is the best predictor (69.1% explained), followed by SM (52.6 %) and P (26.8 %). The more conservative models based on detrended time series further indicate that ER is the best of the three predictors, especially in NH Africa (Figure S12). However, the predictive power of the simplified models decreased substantially, arguably due to the low interannual BA variability in NH Africa, which is problematic when fitting the model to detrended data.

These results point to increased fuel-moisture in humid area as an alternative explanation of the recent decline in BA in Africa. Increased moisture during the FS reduces fuel flammability thereby limiting ignitions and fire spread, particularly in wet savannas (mean annual precipitation >900 mm/year) where moisture is not a limiting factor for vegetation productivity and fuel for fire propagation (Herrmann et al., 2005; N'Datchoh et al., 2015). In the drier savanna of Southern Africa, instead, a positive rainfall-fire relationship is observed: increased moisture in the years before the FS promotes biomass productivity, and hence more dry flammable fuels in the following year (Archibald et al., 2009; Daniau et al., 2013). These results are consistent with previous findings by Andela and van der Werf (2014). Forests in Africa are located within humid and moist subhumid zones that are not fuel-limited, and therefore the negative correlation with climate variables is supported by other studies that found these ecosystems to be sensitive to fire weather and drought (Bedia et al., 2015; Van der Werf et al., 2008).

4. Conclusions

We analyzed recent changes in fire activity in Africa using the 2002–2016 Collection 6 MODIS MCD64A1 Burned Area Product. We observed a strong BA decline in both hemispheres, although trends were only statistically significant in NH. Reductions in cropland BA accounted for approximately one third of the continent-wide decline, but BA declines in natural lands were predominantly associated with climatic conditions, which yielded increased near-surface moisture during 2002–2016. Climate variables that account for near-surface moisture availability antecedent and concurrent to the fire season were the strongest BA predictors. We found that ER explained both the most interannual variability and trend in BA of the three moisture variables considered. Overall, these results show that climate variables can explain a larger portion of the BA decline in Africa compared to previous studies (e.g., Andela & van der Werf, 2014). This outcome may be due to the use of more complex climate variables (EM, SM), to the improved empirical models that use physically meaningful accumulation time intervals, and to the adoption of ecologically relevant spatial analysis units rather than a lattice of square cells (Abatzoglou et al., 2018).

Recent trends in terrestrial moisture may be the result of internal climate variability including El Nino-Southern Oscillation (ENSO) and sea surface temperatures in the tropical Pacific and Indian Oceans (Andela & van der Werf, 2014; Earl & Simmonds, 2017; Rocha & Simmonds, 1997a, 1997b). However, looking at the regional scale, Hulme et al. (2001) established strong forcing of ENSO only in southeastern and eastern equatorial Africa, while Western Africa region with the strongest decline in BA showed little or no rainfall sensitivity to ENSO. Climate model simulations predicted further increase in SM and decrease in drought risk in NH Africa in the second half of the century due to increase in precipitation and/or decrease in evaporative demand (Berg et al., 2017; Lehner et al., 2017). This may imply that current increased fuel moisture is not due to the current cycle of large-scale atmospheric processes, and additional research is needed to attribute the origins of such trends.

We acknowledge several limitations of this study. All input data sets are inherently affected by uncertainties: (i) the accuracy of our cropland mask depends on the LC data set, whose

spatial resolution might be too coarse, especially in very fragmented landscapes; (ii) while MCD64A1 better detects small fires than previous global BA data sets (Giglio et al., 2018), it still underestimates BA in croplands and tropical forests, therefore affecting the confidence of our analysis in these land covers; (iii) despite selecting climate data sets specifically designed and/or validated in Africa, it is well documented that the scarcity of direct observations might cause biases (Akinsanola et al., 2017; Beck, 2017). While the 15-year study period is relatively short for assessing trends, particularly for fire metrics (Parks et al., 2014), the very short fire return intervals in Africa and spatial extents of the ecoregions mitigates the risk of finding spurious correlations. Finally, we note that not in all ecoregions were we able to adequately model BA trends and interannual variability using climate variables alone. This is not unexpected given the numerous other environmental and societal factors influencing fire activity, especially in ecoregions where the majority of BA occurs in croplands, and where it is likely that human activity is the main driver of long-term BA trends. We believe that this research places a high priority on the development of continental scale BA models that assess the impact of both human and climate drivers.

Limitations notwithstanding, our finding of a strong relationship between ER, SM, and BA in most fire-prone ecoregions in Africa provides new insights into the fire-climate relationship in savannas. Although precipitation promotes fuel buildup prior to the fire season, climate variables that incorporate additional meteorological inputs arguably better reflect plant-available moisture, resulting in better predictive ability in a simple linear model.

We believe that this paper work contributes to a growing body of research aimed at better understanding the relationship between anthropogenic pressure, climate, and fire. Our findings suggest that, regardless of the magnitude of human contributions, the role of climate in the changing fire regimes of Africa should not be ignored.

Supplementary Material

Refer to Web version on PubMed Central for supplementary material.

Acknowledgments

This work was supported by NASA awards NNX14AP70A, NNX14AI68G, and 80NSSC18K0400. We thank Michael Humber (UMD) and Tim Link (UI) for the useful suggestions throughout the work. We acknowledge the ESA CCI Land Cover project. We declare no competing interests. The data sets used are public and freely available from their websites: MCD64A1 (https://lpdaac.usgs.gov/dataset_discovery/modis/modis_products_table/mcd64a1_v006); MERRA-2 and FLDAS (https://disc.gsfc.nasa.gov/); LC-CCI (http://maps.elie.ucl.ac.be/CCI/viewer/download.php); TEOW (https://www.worldwildlife.org/publications/terrestrial-ecoregions-of-the-world); Livestock (https://dataverse.harvard.edu/dataset.xhtml?persistentId=doi:10.7910/DVN/GIVQ75); and Road density (https://globio.info).

References

Abatzoglou JT, Williams AP, Boschetti L, Zubkova M, & Kolden CA (2018). Global patterns of interannual climate-fire relationships. Global Change Biology, 24(11), 5164–5175. 10.1111/gcb.14405 [PubMed: 30047195]

Akinsanola AA, Ogunjobi KO, Ajayi VO, Adefisan EA, Omotosho JA, & Sanogo S (2017). Comparison of five gridded precipitation products at climatological scales over West Africa. Meteorology and Atmospheric Physics, 129(6), 669–689. 10.1007/s00703-016-0493-6

Andela N, Morton DC, Giglio L, Chen Y, van der Werf GR, Kasibhatla PS, et al. (2017). A human-driven decline in global burned area. Science, 356(6345), 1356–1362. 10.1126/science.aal4108 [PubMed: 28663495]

Andela N, & van der Werf G (2014). Recent trends in African fires driven by cropland expansion and El Niño to La Niña transition. Nature Climate Change, 4(9), 791–795. 10.1038/nclimate2313

Anderson TM, Ritchie ME, Mayemba E, Eby S, Grace JB, & McNaughton SJ (2007). Forage nutritive quality in the Serengeti ecosystem: The roles of fire and herbivory. The American Naturalist, 170(3), 343–357. 10.1086/520120

Archibald S (2016). Managing the human component of fire regimes: lessons from Africa. Philosophical Transactions of the Royal Society, 371(1696). 10.1098/rstb.2015.0346

Archibald S, & Hempson GP (2016). Competing consumers: contrasting the patterns and impacts of fire and mammalian herbivory in Africa. Philosophical Transactions of the Royal Society Biological Science, 371(1703), 20150309 10.1098/rstb.2015.0309

Archibald S, Lehmann C, Gomez-Dans J, & Bradstock R (2013). Defining pyromes and global syndromes of fire regimes. Proceedings of the National Academy of Sciences, 110(16), 6442–6447. 10.1073/pnas.1211466110

Archibald S, Nickless A, Govender N, Scholes RJ,& Lehsten V (2010). Climate and the inter-annual variability of fire in southern Africa: A meta-analysis using long-term field data and satellite-derived burnt area data. Global Ecology and Biogeography, 19(6), 794–809. 10.1111/j.1466-8238.2010.00568.x

Archibald S, Nickless A, Scholes RJ, & Schulze R (2010). Methods to determine the impact of rainfall on fuels and burned area in southern African savannas. International Journal of Wildland Fire, 19(6), 774–782. 10.1071/WF08207

Archibald S, Roy DP, van Wilgen BW, & Scholes RJ (2009). What limits fire? An examination of drivers of burnt area in Southern Africa. Global Change Biology, 15(3), 613–630. 10.1111/j.1365-2486.2008.01754.x

Archibald S, Scholes RJ, Roy DP, Roberts G, & Boschetti L (2010). Southern African fire regimes as revealed by remote sensing. International Journal of Wildland Fire, 19(7), 861–878. 10.1071/WF10008

Balch JK, Bradley BA, Abatzoglou JT, Nagy RC, Fusco EJ, Mahood AL, & Chelsea Nagy R (2017). Human-started wildfires expand the fire niche across the United States. Proceedings of the National Academy of Sciences, 114(11), 2946–2951. 10.1073/pnas.1617394114

Balfour D, & Howison O (2001). Spatial and temporal variation in a mesic savanna fire regime: responses to variation in annual rainfall. African Journal of Range and Forage Science, 19, 45–53.

Barbero R, Abatzoglou JT, Larkin NK, Kolden CA, & Stocks B (2015). Climate change presents increased potential for very large fires in the contiguous United States. International Journal of Wildland Fire, 24(7), 892–899. 10.1071/WF15083

Beck H (2017). Global-scale evaluation of 22 precipitation datasets using gauge observations and hydrological modeling. Hydrology and Earth System Sciences, 21(12), 6201–6217. 10.5194/hess-21-6201-2017

Bedia J, Herrera S, Gutierrez J, Benali A, Brands S, Mota B, & Moreno JM (2015). Global patterns in the sensitivity of burned area to fire-weather: Implications for climate change. Agricultural and Forest Meteorology, 214-215, 369–379. 10.1016/j.agrformet.2015.09.002

Berg A, Sheffield J, & Milly PCD (2017). Divergent surface and total soil moisture pro)ections under global warming. Geophysical Research Letters, 44, 236–244. 10.1002/2016GL071921

Boschetti L, & Roy DP (2008). Defining a fire year for reporting and analysis of global interannual fire variability. Journal of Geophysical Research, 113, G03020 10.1029/2008JG000686

Bradstock RA (2010). A biogeographic model of fire regimes in Australia: current and future implications. Global Ecology and Biogeography, 19(2), 145–158. 10.1111/j.1466-8238.2009.00512.x

Chatfield C (1996). The analysis of timeseries—An introduction, (5th ed., Vol. 52, p. 1162). London: Chapman and Hall CRC 10.2307/2533084

Cochrane MA (2003). Fire science for rainforests. Nature, 421(6926), 913–919. 10.1038/nature01437 [PubMed: 12606992]

Daniau A-L, Bartlein PJ, Harrison SP, Prentice IC, Brewer S, Friedlingstein P, et al. (2012). Predictability of biomass burning in response to climate changes. Global Biogeochemical Cycles, 26, GB4007 10.1029/2011GB004249

Daniau A-L, Sanchez Goni MF, Martinez P, Urrego DH, Bout-Roumazeilles V, Desprat S, & Marlon JR (2013). Orbital-scale climate forcing of grassland burning in southern Africa. PNAS, 110(13), 5069–5073. 10.1073/pnas.1214292110 [PubMed: 23479611]

Dembele M, & Zwart SJ (2016). Evaluation and comparison of satellite-based rainfall products in Burkina Faso, West Africa. International Journal of Remote Sensing, 37(17), 3995–4014. 10.1080/01431161.2016.1207258

Dinku T, Hailemariam K, Maidment R, Tarnavsky E, & Connor S (2014). Combined use of satellite estimates and rain gauge observations to generate high-quality historical rainfall time series over Ethiopia. International Journal of Climatology, 34(7), 2489–2504. 10.1002/joc.3855

Durbin J, & Watson GS (1950). Testing for serial correlation in least squares regression I. Biometrika, 37(3-4), 409–428. [PubMed: 14801065]

Earl N, & Simmonds I (2017). Variability, trends, and drivers of regional fluctuations in Australian fire activity. Journal of Geophysical Research: Atmospheres, 122, 7445–7460. 10.1002/2016JD026312

Earl N, & Simmonds I (2018). Spatial and temporal variability and trends in 2001–2016 global fire activity. Journal of Geophysical Research: Atmospheres, 123, 2524–2536. 10.1002/2017JD027749

Funk C, Peterson P, Landsfeld M, Pedreros D, Verdin J, Shukla S, et al. (2015). The climate hazards infrared precipitation with stations—A new environmental record for monitoring extremes. Scientific Data, 2(1), 150066 10.1038/sdata.2015.66 [PubMed: 26646728]

Giglio L, Boschetti L, Roy D, Hoffmann AA, & Humber M (2016). Collection 6 MODIS burned area product user's guide version 1.0.

Giglio L, Boschetti L, Roy DP, Humber ML, & Justice CO (2018). The Collection 6 MODIS burned area mapping algorithm and product. Remote Sensing of Environment, 217, 72–85. 10.1016/j.rse.2018.08.005 [PubMed: 30220740]

Giglio L, Randerson JT, & van der Werf GR (2013). Analysis of daily, monthly, and annual burned area using the fourth-generation global fire emissions database (GFED4). Journal of Geographical Research: Biogeoscience, 118, 317–328. 10.1002/jgrg.20042

Gilbert M, Nicolas G, Cinardi G, Van Boeckel TP, Vanwambeke SO, Wint GRW, & Robinson TP (2018). Global distribution data for cattle, buffaloes, horses, sheep, goats, pigs, chickens and ducks in 2010. Scientific Data, 5,180227 10.1038/sdata.2018.227 [PubMed: 30375994]

Herrmann SM, Anyamba A, & Tucker CJ (2005). Recent trends in vegetation dynamics in the African Sahel and their relationship to climate. Global Environmental Change, 15(4), 394–404. 10.1016/j.gloenvcha.2005.08.004

Higuera PE, Abatzoglou JT, Littell JS, & Morgan P (2015). The changing strength and nature of fire-climate relationships in the northern Rocky Mountains, U.S.A., 1902-2008. PLoS ONE, 10(6), e0127563 10.1371/journal.pone.0127563 [PubMed: 26114580]

Hoscilo A, Balzter H, Bartholome E, Boschetti M, Brivio PA, Brink A, et al. (2014). A conceptual model for assessing rainfall and vegetation trends in sub-Saharan Africa from satellite data. International Journal of Climatology, 35(12), 3582–3592. 10.1002/joc.4231

Hulme M, Doherty R, Ngara T, New M, & Lister D (2001). African climate change: 1900-2100. Climate Research, 17, 145–168.10.3354/cr017145

James G, Witten D, Hastie T, & Tibshirani R (2013). An introduction to statistical learning: with applications in R. New York: Springer Publishing Company, Incorporated 10.1007/978-1-4614-7138-7

Knowles T, Assede E, Daitz D, Geldenhuys C, Scholes R, Trollope WSW, et al. (2016). Africa—The fire continent: fire in contemporary African landscapes Report. World Bank Group.

Le Page Y, Oom D, Silva J, Jonsson P, & Pereira J (2010). Seasonality of vegetation fires as modified by human action: observing the deviation from eco-climatic fire regimes. Global Ecology and Biogeography, 19, 575–588. 10.1111/j.1466-8238.2010.00525.x

Lehmann CE, Anderson TM, Sankaran M, Higgins SI, Archibald S, Hoffmann WA, et al. (2014). Savanna vegetation-fire-climate relationships differ among continents. Science, 343(6170), 548–552. 10.1126/science.1247355 [PubMed: 24482480]

Lehner F, Coats S, Stocker TF, Pendergrass AG, Sanderson BM, Raible CC, & Smerdon JE (2017). Projected drought risk in 1.5°C and 2°C warmer climates. Geophysical Research Letters, 44, 7419–7428. 10.1002/2017GL074117

Littell JS, Peterson D, Riley K, Liu Y, & Luce C (2016). A review of the relationships between drought and forest fire in the United States. Global Change Biology, 22(7), 2353–2369. 10.1111/gcb.13275 [PubMed: 27090489]

McNally A, Arsenault K, Kumar S, Shukla S, Peterson P, Wang S, et al. (2017). A land data assimilation system for sub-Saharan Africa food and water security applications. Nature Scientific Data, 4(1), 170012 10.1038/sdata.2017.12

Meijer JR, Huijbegts MAJ, Schotten CGJ, & Schipper AM (2018). Global patterns of current and future road infrastructure. Environmental Research Letters, 13(6). 10.1088/1748-9326/aabd42

Moritz MA, Parisien M-A, Batllori E, Krawchuk MA, van Dorn J, & Ganz DJ (2012). Climate change and disruptions to global fire activity. Ecosphere, 3(6), 1–22. 10.1890/ES11-00345.1

Murphy BP, Williamson GJ, & Bowman DM (2011). Fire regimes: moving from a fuzzy concept to geographic entity. New Phytologist, 192(2), 316–318. 10.1111/j.1469-8137.2011.03893.x [PubMed: 21950336]

N'Datchoh E, Konare A, Diedhiou A, Diawara A, Quansah E, & Assamoi P (2015). Effects of climate variability on savannah fire regimes in West Africa. Earth System Dynamics, 6(1), 161–174. 10.5194/esd-6-161-2015

Olson DM, Dinerstein E, Wikramanayake ED, Burgess ND, Powell GVN, Underwood EC, et al. (2001). Terrestrial Ecoregions of the World: A New Map of Life on Earth. BioScience, 51(11), 933–938. 10.1641/0006-3568(2001)051[0933:TEOTWA]2.0.CO;2

Parks SA, Parisien M-A, Miller C, & Dobrowski SZ (2014). Fire activity and severity in the western US vary along proxy gradients representing fuel amount and fuel moisture. PLoS ONE, 9(6), e99699 10.1371/journal.pone.0099699 [PubMed: 24941290]

Pica-Ciamarra U, Otte J, & Chilonda P (2007). Livestock policies, land and rural conflicts in sub-Saharan Africa. Africa, 07,1–20.

Rabin SS, Magi BI, Shevliakova E, & Pacala SW (2015). Quantifying regional, time-varying effects of cropland and pasture on vegetation fire. Biogeosciences, 12(22), 6591–6604. 10.5194/bg-12-6591-2015

Rienecker MM, Suarez MJ, Gelaro R, Todling R, Bacmeister J, Liu E, et al. (2011). MERRA: NASA's modern-era retrospective analysis for research and applications. Journal of Climate, 24(14), 3624–3648. 10.1175/JCLI-D-11-00015.1

Riley KL, Abatzoglou JT, Grenfell IC, Klene AE, & Heinsch FA (2013). The relationship of large fire occurrence with 15 drought and fire danger indices in the western USA, 1984 – 2008: The role of temporal scale. International Journal of Wildland Fire, 22(7), 894–909. 10.1071/WF12149

Rocha A, & Simmonds I (1997a). Interannual variability of south-eastern African summer rainfall: Part I. Relationships with air-sea interaction processes. International Journal of Climatology, 17, 235–265.

Rocha A, & Simmonds I (1997b). Interannual variability of south-eastern African summer rainfall: Part II. Modelling the impact of sea-surface temperatures on rainfall and circulation. International Journal of Climatology, 17, 267–290.

Rodell M, Famiglietti JS, Wiese DN, Reager JT, Beaudoing HK, Landerer FW, & Lo MH (2018). Emerging trends in global freshwater availability. Nature, 557(7707), 651–659. 10.1038/s41586-018-0123-1 [PubMed: 29769728]

Tadesse T, Demisse GB, Zaitchik B, & Dinku T (2014). Satellite-based hybrid drought monitoring tool for prediction of vegetation condition in eastern Africa: A case study for Ethiopia. Water Resources Research, 50, 2176–2190. 10.1002/2013WR014281

Toté C, Patricio D, Boogaard H, van der Wijngaart R, Tarnavsky E, & Funk C (2015). Evaluation of satellite rainfall estimates for drought and flood monitoring in Mozambique. Remote Sensing, 7(2), 1758–1776. 10.3390/rs70201758

Van der Werf GR, Randerson JT, Giglio L, Gobron N, & Dolman AJ (2008). Climate controls on the variability of fires in the tropics and subtropics. Global Biogeochem Cycles, 22, GB3028 10.1029/2007GB003122

Van der Werf GR, Randerson JT, Giglio L, Van Leeuwen TT, Chen Y, Rogers BM, et al. (2017). Global fire emissions estimates during 1997-2016. Earth System Science Data, 9(2), 697–720. 10.5194/essd-9-697-2017

Van Wilgen BW, Govender N, Biggs HC, Ntsala D, & Funda XN (2004). Response of savanna fire regimes to changing fire-management policies in a large African national park. Conservation Biology, 18(6), 1533–1540. 10.1111/j.1523-1739.2004.00362.x

Van Wilgen BW, & Scholes RJ (1997). The vegetation and fire regimes of southern-hemisphere Africa In van Wilgen BW, Andreae MO, Goldammer JG, & Lindesay JA (Eds.), Fire in southern African savannas: Ecological and atmospheric perspectives (pp. 27–46). Johannesburg: Witwatersrand University Press.

Williams AP, & Abatzoglou JT (2016). Recent advances and remaining uncertainties in resolving past and future climate effects on global fire activity. Current Climate Change Reports, 2(1), 1–14. 10.1007/s40641-016-0031-0

Wooldridge M (2013). Introductory econometrics: A modern approach (5th ed.). Mason: South-Western.

Zhao M, & Running S (2010). Drought-induced reduction in global terrestrial net primary production from 2000 through 2009. Science, 329(5994), 940–943. 10.1126/science.1192666 [PubMed: 20724633]

References From the Supporting Information

CCI-LC-PUGV2 (2017). Land cover CCI product user guide version 2.0. Retrieved from http://maps.elie.ucl.ac.be/CCI/viewer/download/ESACCI-LC-Ph2-PUGv2_2.0.pdf

Key Points:

- Burned area in Africa declined by 18.5% (51.9 Mha) from 2002–2016
- The majority of the decline (35.4 Mha) occurred in noncropland areas
- 71.2% of the decline in noncropland burned area can be explained by changes in effective rainfall

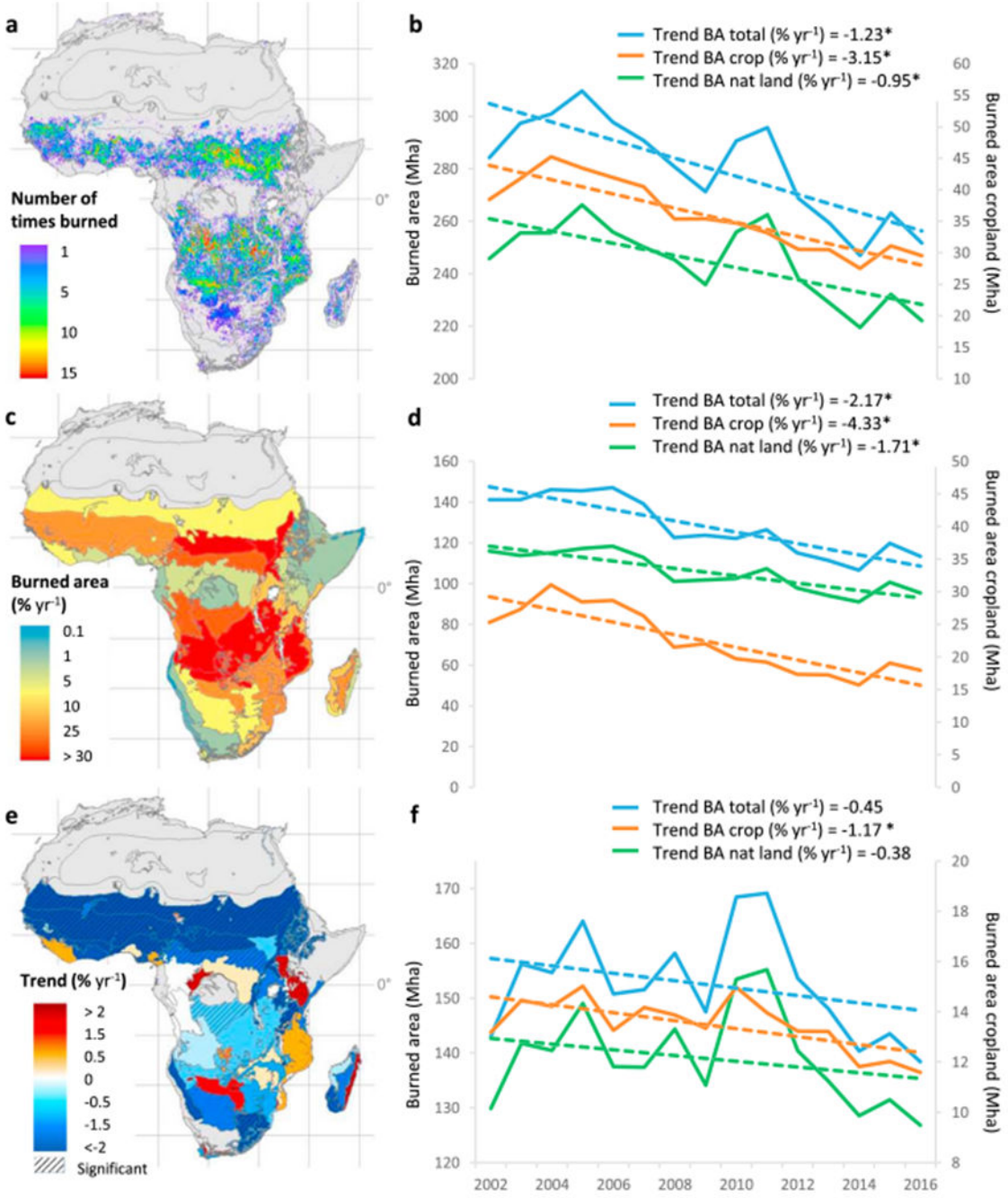

Figure 1.

Left column: (a) Number of times burned during in the 2002–2016 study period (at MODIS 500-m resolution); (c) average ecoregion burned area fraction per year; (e) linear trends in burned area. Gray color represents ecoregions with negligible fire activity (less than 0.5% of the ecoregion burned on average). Graticule lines are every 10°. Right column: Burned area time series observed by MCD64A1 for (b) whole continent; (d) Northern Hemisphere; (f) Southern Hemisphere. In all three cases, the plots report the total burned area (blue lines), the burned area detected in croplands (orange lines) and the burned area detected in natural

lands (green lines), with the respective trends represented by the dashed lines. Asterisk indicates significant trends.

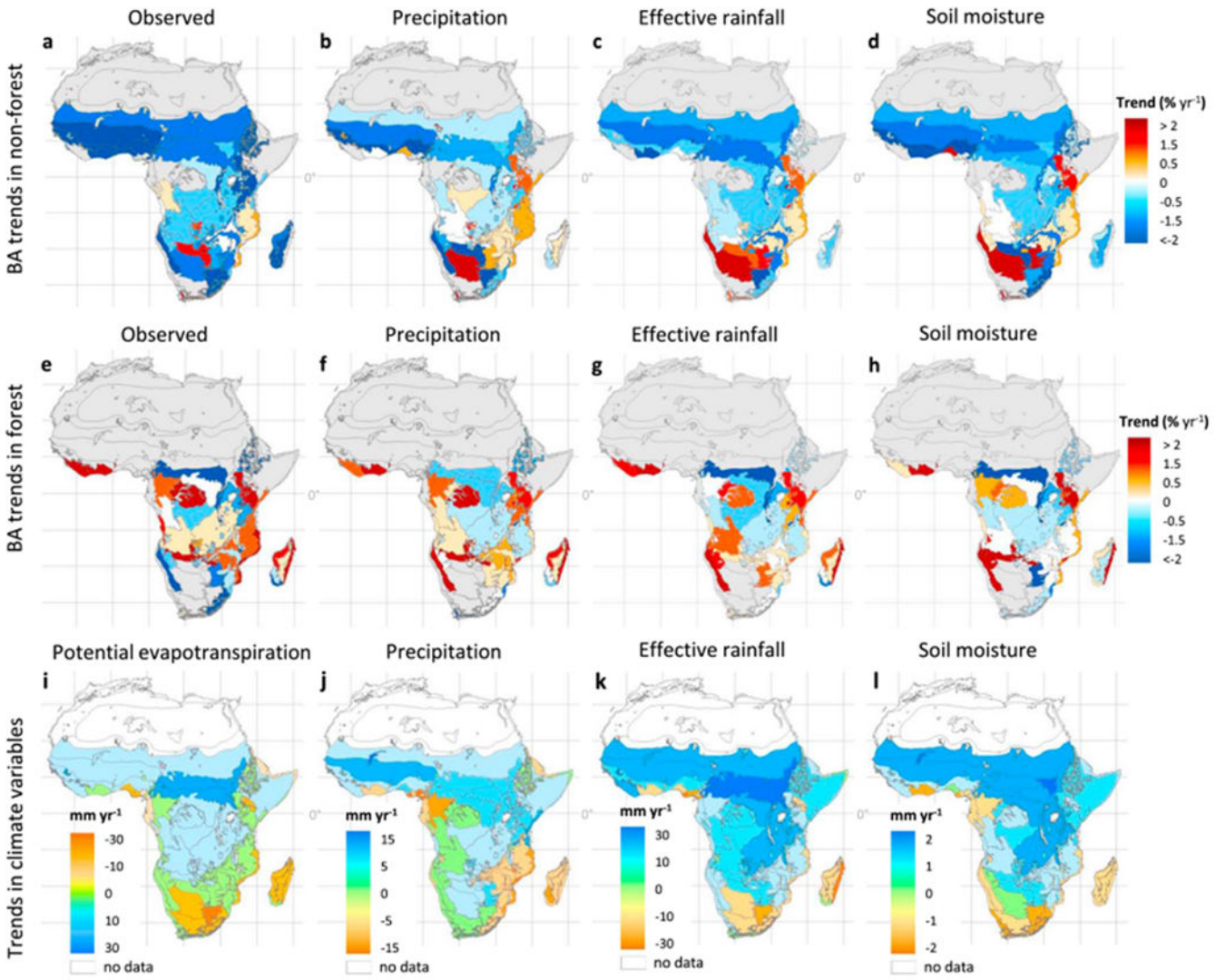

Figure 2.

Linear trends in burned area and climate data. Top row, (a–d) Burned area (BA) trends in nonforest; middle row (e–h) BA trend in forest; bottom row (i–l) trends of climate variables. (a, e) Observed linear trend in burned area; (b, f) modeled linear trends using precipitation as a predictor; (c, g) modeled linear trends using effective rainfall as a predictor; (d, h) modeled linear trends using soil moisture as a predictor. Gray color represents ecoregions with negligible fire activity in each land cover. Graticule lines are every 10°.

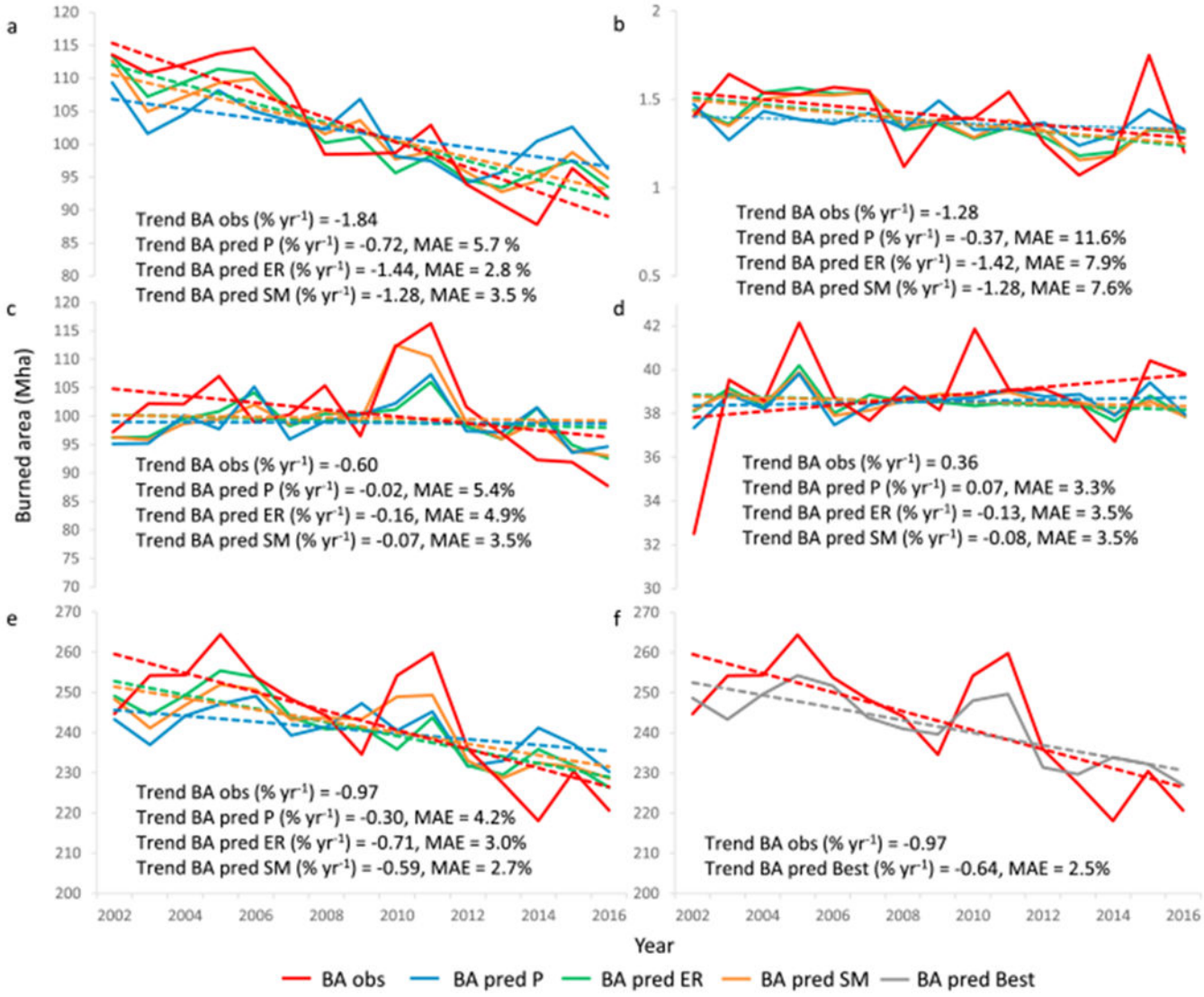

Figure 3.

Observed and predicted burned area (BA) in natural lands. Linear trends in (a) Northern Hemisphere nonforest; (b) Northern Hemisphere forest; (c) Southern Hemisphere nonforest; (d) Southern Hemisphere forest; (e) the whole continent; (f) the whole continent, selecting in each ecoregion the model with the highest adjusted R2 (Figure S6 in the supporting information). (BA obs = burned area observed from MODIS MCD64A1; BA pred = burned area predicted by linear models; model was computed with precipitation as predictor; ER = effective rainfall; SM = soil moisture; MAE = mean absolute error as a percent of the average BA obs).